

AGAPE, a microlensing search in the direction of M31: status report

R. Ansari^a, M. Aurière^b, P. Baillon^c, A. Bouquet^{d,f}, G. Coupinot^b,
C. Coutures^e, C. Ghesquière^f, Y. Giraud-Héraud^f, P. Gondolo^{d,g}, J. Hecquet^b,
J. Kaplan^{d,f}, Y. Le Du^f, A.L. Melchior^f, M. Moniez^a, J.P. Picat^b,
and G. Soucail^b

^a *LAL, Université Paris Sud, Orsay, France,*

^b *Observatoire Midi-Pyrénées Bagnères de Bigorre et Toulouse, France,*

^c *CERN, Genève, Switzerland,* ^d *LPTHE, Universités Paris 6 et 7, France,*

^e *DAPNIA, CEN Saclay, France,* ^f *LPC Collège de France, Paris, France.*

^g *Theoretical Physics, University of Oxford, United Kingdom*

Presented at the second Workshop : “The dark side of the Universe : experimental efforts
and theoretical framework” Roma 13-14 November 1995, by J. Kaplan.

LPC 96-04/conf

The M31 galaxy in Andromeda is the nearest large galaxy after the Small and Large Magellanic Clouds. It is a giant galaxy, roughly 2 times as large as our Milky Way, and has its own halo. As pointed by some of us [1, 2] and independantly by A. Crots [3], M31 provides a rich field of stars to search for MACHO's in galactic halos by gravitational microlensing [4]. M31 is a target complementary to the Magellanic Clouds used by the current experiments [5, 6]. It is complementary in that it allows to probe the halo of our galaxy in a direction very different from that of the LMC. Moreover, the fact that M31 has its own halo and is tilted with respect to the line of sight provides a very interesting signature [3] : assuming an approximately spherical halo for M31, the far side of the disk lies behind a larger amount of M31 dark matter, therefore more microlensing events are expected on the far side of the disk. Such an asymmetry could not be faked by variable stars.

In other words, M31 seems very appropriate to detect brown dwarfs through microlensing. However, as very few stars of M31 are resolved, we had to develop a new approach to look for microlensing by monitoring the pixels of a CCD, rather than individual stars [1, 2]. The AGAPE collaboration has set out to implement this idea.

Monitoring pixels

In the case of a crowded field such as M31, the light flux F_{pixel} on a pixel comes from the many stars in and around it, plus the sky background. The light flux of an individual star, F_{star} , is spread among all pixels of the seeing spot and only a fraction of this light, $F_{\text{pixel}} = \{\text{seeing fraction}\} \times F_{\text{star}}$, reaches the central pixel. If the star luminosity is amplified by a factor A , the pixel flux increases by :

$$\Delta F_{\text{pixel}} = (A - 1) \{\text{seeing fraction}\} F_{\text{star}} . \quad (1)$$

The amplification of the star luminosity allows an event to be detected if the flux on the brightest pixel rises sufficiently high above its rms fluctuation σ_{pixel} :

$$\Delta F_{\text{pixel}} > Q \sigma_{\text{pixel}} . \quad (2)$$

Typically, in our simulations, we require Q to be larger than 3 during 3 consecutive exposures and larger than 5 for at least one of them.

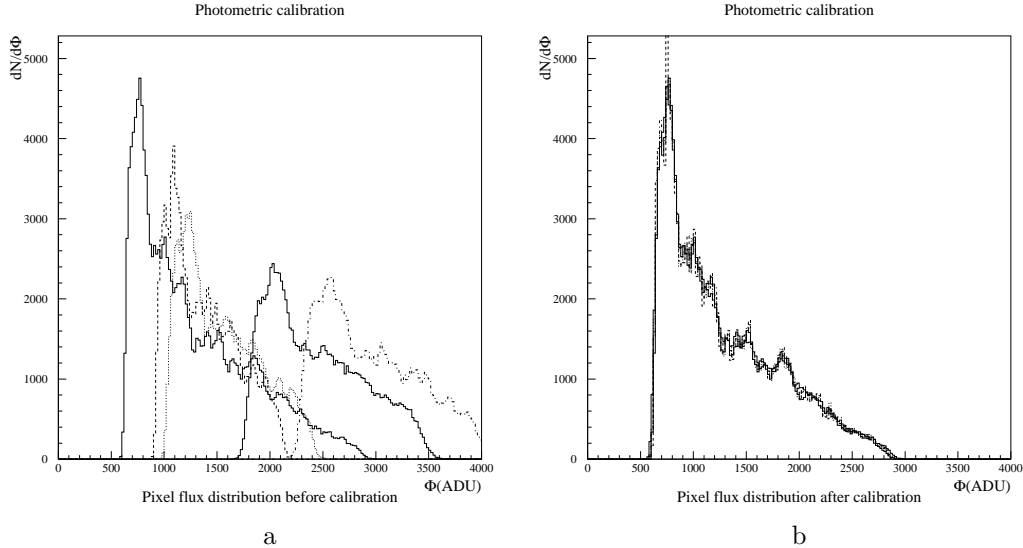


Figure 1: The matching of pixel histograms before (a) and after (b) photometric alignment

All our simulations [1, 2, 7] indicate that the statistics should be significant if the relative fluctuation of the current pixels (i.e. where no particular activity occurs) can be made sufficiently small. This crucial point is the first step of our data analysis and is discussed in detail below.

Status of the analysis

We took data during 60 nights of observation on the 2 meter “Bernard Lyot” telescope at Observatoire du Pic du Midi in the French Pyrénées, from September 29 to November 24 in 1994, and 93 nights, from July 28 to Dec 31 in 1995. Of these 153 nights, only 61 came out with good weather. The field regularly covered was $8' \times 8'$, with 4 exposures on a 800×800 part of a thin Tektronix CCD camera with pixels $0.3''$ wide. Two other $4' \times 4'$ fields were occasionally covered.

Images have been taken with both red (Gunn) and blue (Johnson) filters, but less regularly in blue. We have not yet started the analysis of the blue frames.

Geometrical alignment. A definite pixel never points exactly in the same direction of the sky on two different exposures. Successive images have therefore to be realigned geometrically by software, in order that the light curve of a pixel really represents the light curve of a definite region of the sky. To this aim, we match the positions of bright stars between the current image and a reference image, using an adaptation to our case of the program PEIDA devised by the EROS collaboration [8]. The precision of the geometrical realignment thus obtained is better than 0.3 pixel ($0.1''$). Such a precision is fully satisfactory, as we construct our light curves on super-pixels of size 5 pixel \times 5 pixel or larger.

Photometric alignment. The sky background light and the atmospheric absorption differ from one picture to the other. Before any photometric follow-up, it is necessary to correct for these differences. We do that by matching the dispersion and the mean value of the histogram of pixel intensities between each frame and a reference one. This method works well in this case because the local luminosity gradient in M31 largely supersedes all other sources of dispersion. Figure 1 shows how well pixel histograms, that look very different before treatment, coincide up to small structures after a renormalization by only two parameters : an overall multiplicative factor for the atmospheric absorption and an additive constant for the sky background. To check the quality of the photometric alignment obtained, we eval-

AGAPE - A field - seeing $1.8''$ - 1994-1995

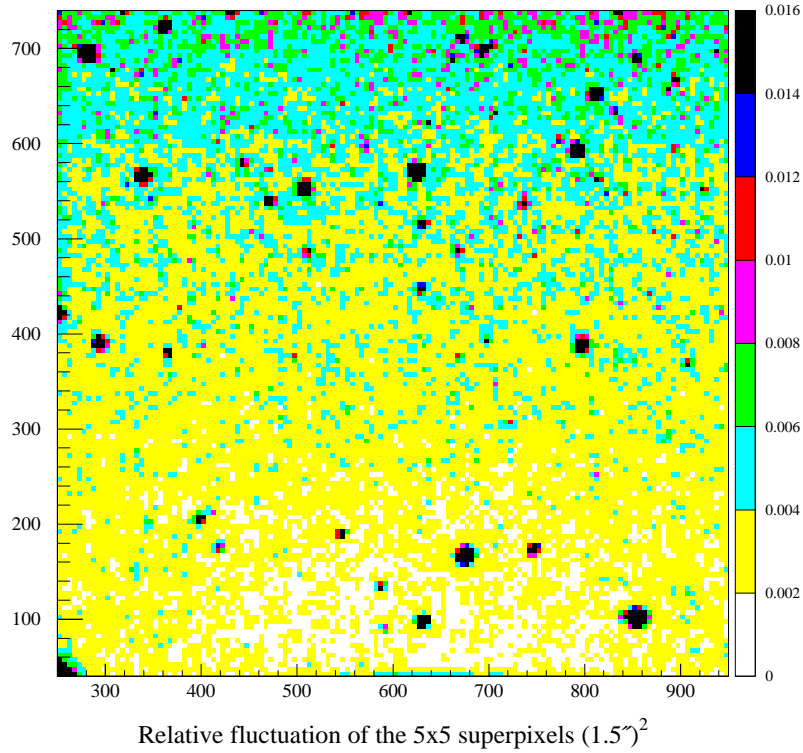


Figure 2: The relative fluctuation on field A

uated the relative intensity fluctuation of each super-pixel among all exposures. Figure 2 shows a map of this relative dispersion for 5×5 super-pixels for one of our fields. We see that this dispersion does not exceed 0.5% on most of the field, which is around twice the photon noise. This can be looked at in a different way (figure 3): after constructing a light

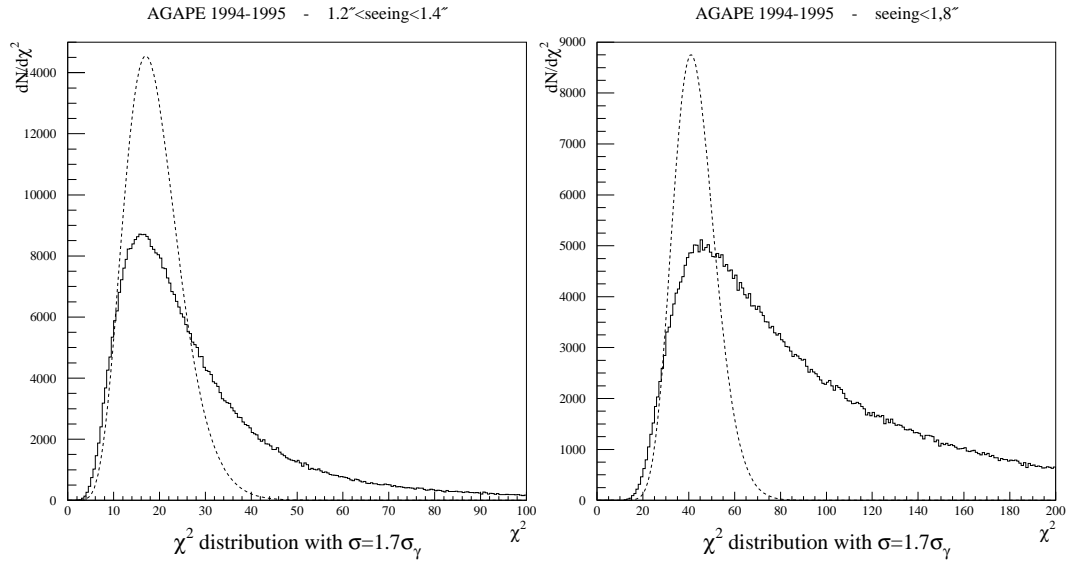


Figure 3: The relative fluctuation on field A

curve for each super-pixel, one can compute along each light curve the χ^2 of the intensity compared with its average. On figure 3, we display for two different seeing intervals the distribution of this χ^2 . The error σ entering the χ^2 is chosen in such a way that the maximum of the distribution coincides with that of the ideal poissonnian χ^2 distribution. The true distributions show non poissonnian tails. Clearly there are non gaussian contributions to the fluctuations and a comparison between figure 3a and 3b shows that they are largely due to seeing variations. Further work is in progress to cope with seeing variations.

Present results.

Let us exemplify the kind of results we get by the light curve of a 7×7 super-pixel shown

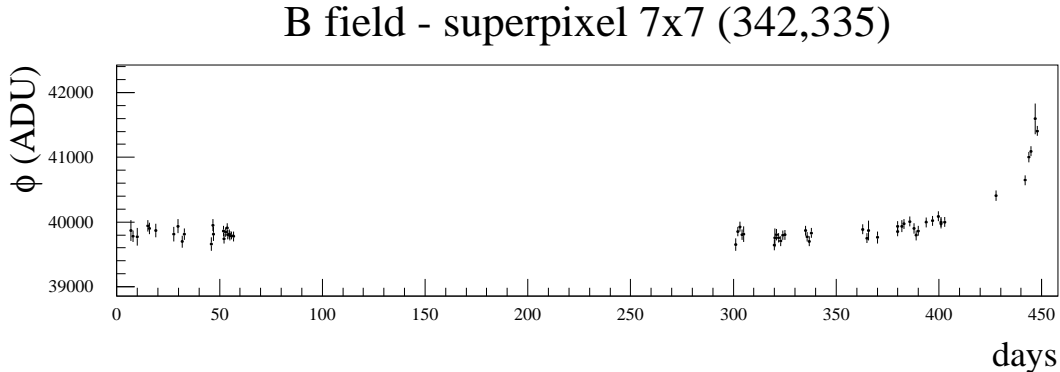


Figure 4: A typical light curve

on figure (4). This light curve first shows the degree of stability ($\simeq 0.5\%$) we achieve on a stable pixel. It appears consistent with error bars taken as twice the photon noise as explained earlier. A second point apparent on this light curve is that a magnitude variation $\Delta m \simeq 0.02$ (800/40000 ADU) of the super-pixel is clearly detectable.

Figure 5 shows another light curve. On graph 5a all frames are retained, whereas only frames with seeing between $1.2''$ and $1.8''$ are kept in graph 5b. This illustrates the instabilities introduced by seeing variations. However, when extreme seeing have been excluded (graph 5b), a magnitude change $\Delta m \simeq 0.015$ is clearly detected. There are two luminosity variations, therefore it is not a microlensing event.

Plots 5c and 5d display the intensity in a square of side 30 elementary pixels ($10''$). The hills in the landscape are structures of M31 and appear in the same way on both plots. However, a tiny hill at the center of plot 5c has grown to a high peak on plot 5d. The clear point-spread-function shape of the growing peak tells us that we are really looking at the variation of the luminosity of a star. This is confirmed by the progressive rise and fall of this peak on exposures before and after the maximum shown on plot 5d. Clearly, such a faint variable object would not have been detected by monitoring resolved stars.

We have a catalog of a few hundred such variations, most of which are multiple and therefore are not microlensing events. We are now working i) to treat the seeing variations ii) to interpret the variations we see in terms of known types of variable stars, iii) to try and isolate events compatible with microlensing and in any case to evaluate our sensitivity threshold for the detection of microlensing events.

We thank professor A. Gould for useful discussions and suggestions.

References

D field - superpixel 7x7 (693,182)

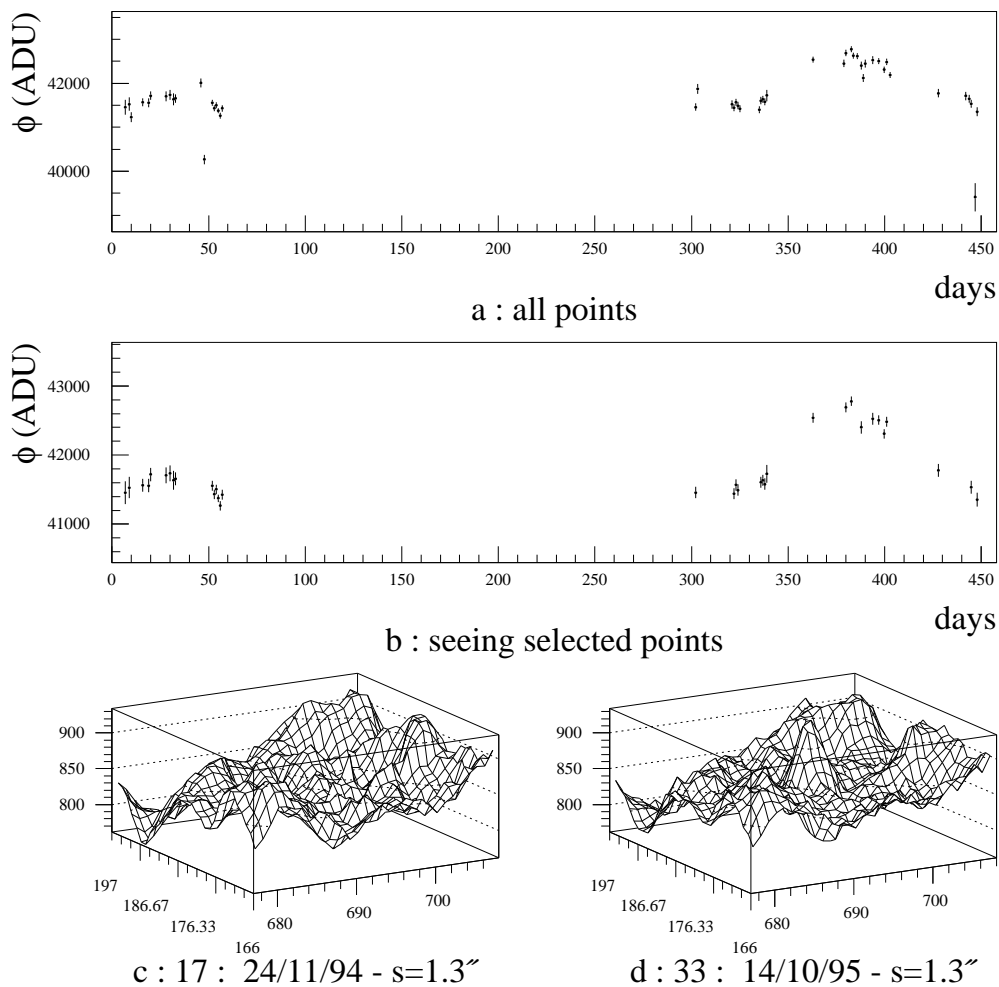


Figure 5: Another typical light curve

- [1] Baillon P. Bouquet A. Giraud-Héraud Y. & Kaplan J. 1992. "Search for dark matter as brown dwarves by looking at Andromeda (M31)", Proceedings of the first Palaiseau Workshop, Fleury P. Vacanti G. editors, Edition Frontières 1992; p151.
- [2] Baillon P. Bouquet A. Giraud-Héraud Y. & Kaplan J. 1993. A&A 277; 1.
- [3] Crofts A. P. S. 1992. ApJ. 399; L43.
- [4] Paczyński B. 1986. ApJ. 304; 1.
- [5] Alcock et al., 1993. Nature 365; 621, and these proceedings.
- [6] Aubourg E. et al. 1993. Nature 365; 623.
- [7] Ansari et al. 1995. 17th Texas symposium on relativistic astrophysics and cosmology, Annals of the New York academy of sciences 759; 608.
- [8] "Programme de reconstruction photométrique PEIDA Version V", 1995. EROS technical note.